

การวิเคราะห์สมบัติทางไดรโบลอยีของสารหล่อลื่นสำหรับการจัดในกระบวนการผลิตฮาร์ดดิสก์



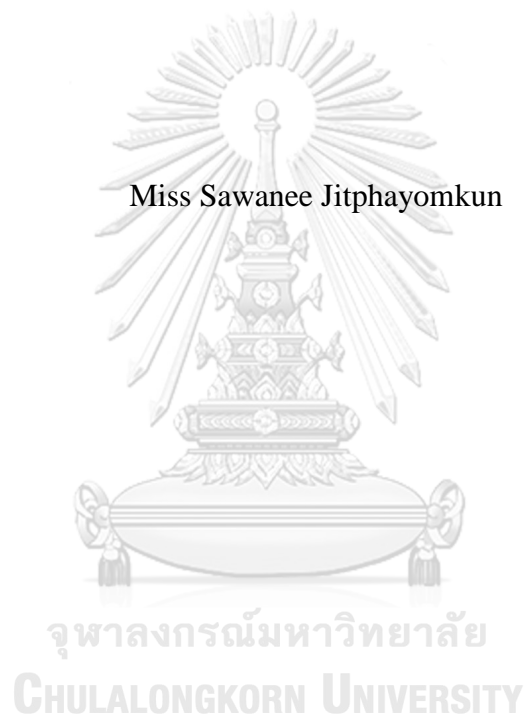
บทคัดย่อและแฟ้มข้อมูลฉบับเต็มของวิทยานิพนธ์ตั้งแต่ปีการศึกษา 2554 ที่ให้บริการในคลังปัญญาจุฬาฯ (CUIR)  
เป็นแฟ้มข้อมูลของนิสิตเจ้าของวิทยานิพนธ์ ที่ส่งผ่านทางบัณฑิตวิทยาลัย

The abstract and full text of theses from the academic year 2011 in Chulalongkorn University Intellectual Repository (CUIR)  
are the thesis authors' files submitted through the University Graduate School.

วิทยานิพนธ์นี้เป็นส่วนหนึ่งของการศึกษาตามหลักสูตรปริญญาวิทยาศาสตรมหาบัณฑิต  
สาขาวิชาฟิสิกส์ ภาควิชาฟิสิกส์  
คณะวิทยาศาสตร์ จุฬาลงกรณ์มหาวิทยาลัย  
ปีการศึกษา 2560  
ลิขสิทธิ์ของจุฬาลงกรณ์มหาวิทยาลัย

TRIBOLOGICAL CHARACTERIZATION OF LAPPING LUBRICANT IN HARD  
DISK DRIVE FABRICATION

Miss Sawanee Jitphayomkun



A Thesis Submitted in Partial Fulfillment of the Requirements  
for the Degree of Master of Science Program in Physics  
Department of Physics  
Faculty of Science  
Chulalongkorn University  
Academic Year 2017  
Copyright of Chulalongkorn University

Thesis Title                           TRIBOLOGICAL CHARACTERIZATION OF  
LAPPING LUBRICANT IN HARD DISK  
DRIVE FABRICATION

By   Miss Sawanee Jitphayomkun

Field of Study                           Physics

Thesis Advisor                         Assistant Professor Sukkaneste Tungasmita,  
Ph.D.

---

Accepted by the Faculty of Science, Chulalongkorn University in Partial  
Fulfillment of the Requirements for the Master's Degree

.....Dean of the Faculty of Science  
(Associate Professor Polkit Sangvanich, Ph.D.)

**THESIS COMMITTEE**

.....Chairman  
(Assistant Professor Rattachat Mongkolnavin, Ph.D.)

.....Thesis Advisor  
(Assistant Professor Sukkaneste Tungasmita, Ph.D.)

.....Examiner  
(Assistant Professor Panadda Dechadilok, Ph.D.)

.....External Examiner  
(Chakkrit Supavasuthi)

สวนีย์ จิตต์พยอมกุล : การวิเคราะห์สมบัติทางไตรโบโลยีของสารหล่อลื่นสำหรับการจัด  
 ในกระบวนการผลิตฮาร์ดดิสก์ (TRIBOLOGICAL CHARACTERIZATION OF  
 LAPPING LUBRICANT IN HARD DISK DRIVE FABRICATION) อ.ที่  
 ปรักษาวิทยานิพนธ์หลัก: ผศ. ดร. สุกคณศ ตุงคะสมิต, 36 หน้า.

ในกระบวนการผลิตฮาร์ดดิสก์ขั้นตอนที่สำคัญขั้นตอนหนึ่งคือกระบวนการขัดผิวหน้า  
 ของหัวอ่านเขียน การสัมผัสกันของวัตถุสองชนิดขึ้นไปก่อให้เกิดแรงเสียดทาน และผลของแรง  
 เสียดทานนี้ทำให้ผิวหน้าของวัตถุที่มีความแข็งน้อยกว่าถูกขัดออกไป การเติมสารหล่อลื่นเข้าไปใน  
 ขั้นตอนการขัดนอกจากจะช่วยลดแรงเสียดทานระหว่างผิวสัมผัสแล้ว สารหล่อลื่นยังช่วยถ่ายเท  
 ความร้อนออกจากระบบและช่วยดักจับเศษของผิวชิ้นงานที่ถูกขัดอีกด้วย โดยงานวิจัยชิ้นนี้มุ่งศึกษา  
 ผลของการเปลี่ยนแปลงตัวแปรทางไตรโบโลยีต่อลักษณะของสารหล่อลื่น โดยใช้เครื่องไตรโบ  
 มิเตอร์แบบบอลออนดิสก์ พฤติกรรมทางไตรโบโลยีของสารหล่อลื่นที่มีฐานต่างชนิดกันได้  
 ถูกนำมาศึกษาเปรียบเทียบภายใต้เงื่อนไขเดียวกันกับในกระบวนการขัดจริงของหัวอ่านเขียน พบว่า  
 สารหล่อลื่นพื้นฐานเอทิลีนไกลคอลและสารหล่อลื่นพื้นฐานปิโตรเลียมในค่าเฉลี่ยสัมประสิทธิ์  
 ความเสียดทาน (คิดหลังจากรอบการสัมผัสที่ 100) อยู่ที่  $0.089 \pm 0.115$  และ  $0.023 \pm 0.012$   
 ตามลำดับ ซึ่งค่าสัมประสิทธิ์ความเสียดทานของสารหล่อลื่นทั้งสองชนิดนี้มีค่าต่ำกว่าสัมประสิทธิ์  
 ความเสียดทานในระบบที่ไม่มีสารหล่อลื่นมาก นอกจากนี้ภาพที่ได้จากกล้องจุลทรรศน์อิเล็กตรอน  
 แบบส่องกราดพิสูจน์ให้เห็นว่ารอยการสึกหรอที่เกิดขึ้นในระบบที่ไม่มีสารหล่อลื่นเกิดกว้างและลึก  
 กว่าในระบบที่ใส่สารหล่อลื่น การเปลี่ยนแปลงแรงกดในแนวตั้งฉากและความเร็วโกลไม่ส่งผลต่อ  
 ระบบที่ไม่มีสารหล่อลื่นมากนัก โดยที่ระบบที่ไม่มีสารหล่อลื่นนี้อยู่ในสภาวะการหล่อลื่นแบบบาวน์  
 ดารี ในทางตรงกันข้ามการเพิ่มแรงกดในแนวตั้งฉากเปลี่ยนสภาวะการหล่อลื่นแบบกึ่งสมบูรณ์เป็น  
 สภาวะการหล่อลื่นแบบบาวน์ดารีในสารหล่อลื่นพื้นฐานน้ำมัน แต่ทั้งแรงกดตั้งฉากและความเร็วมี  
 ผลต่อสารหล่อลื่นพื้นฐานเอทิลีนไกลคอล โดยที่แรงกดตั้งฉาก 0.1 นิวตัน มีการเปลี่ยนสภาวะการ  
 หล่อลื่นแบบกึ่งสมบูรณ์ในความเร็วต่ำ เป็นแบบสมบูรณ์ในความเร็วที่สูงขึ้น แต่ที่แรงกด 0.5 นิว  
 ตัน มีการเปลี่ยนสภาวะการหล่อลื่นแบบกึ่งสมบูรณ์ในความเร็วต่ำเป็นแบบบาวน์ดารีในความเร็วที่  
 สูงขึ้น นอกจากนี้ยังได้มีการศึกษาผลของสารเติมแต่งในสารหล่อลื่นพื้นฐานเอทิลีนไกลคอล พบว่า  
 สารเติมแต่งประเภทสารลดแรงตึงผิวมีสภาวะการหล่อลื่นแบบบาวน์ดารี และประเภทสารป้องกันการ  
 การกัดกร่อนมีสภาวะการหล่อลื่นแบบกึ่งสมบูรณ์

ภาควิชา ฟิสิกส์

ลายมือชื่อนิสิต .....

สาขาวิชา ฟิสิกส์

ลายมือชื่อ อ.ที่ปรึกษาหลัก .....

ปีการศึกษา 2560

# # 5772176723 : MAJOR PHYSICS

KEYWORDS: BALL-ON-DISK TRIBOMETER / FRICTION REGIMES / HARD DISK DRIVE (HDD) / LUBRICANT

SAWANEE JITPHAYOMKUN: TRIBOLOGICAL CHARACTERIZATION OF LAPPING LUBRICANT IN HARD DISK DRIVE FABRICATION.  
ADVISOR: ASST. PROF. SUKKANESTE TUNGASMITA, Ph.D., 36 pp.

One of the most important processes in hard disk drive fabrication is the lapping process. As two bodies are in contact, the friction occurs, and the softer material can be worn out by the harder. By using lubricant in the lapping process, it does not only reduce the friction, but it also transfers heat and captures debris away from the surface contacts. This thesis work focused on the effects of tribological parameters toward the characteristics of lubricants, using ball-on-disk tribometer. The tribological behaviors between using different base lubricants were investigated. At the same condition as final lapping process, EG-based and oil-based lubricants exhibited the average coefficient of friction (after 100 contact cycles) at about  $0.089 \pm 0.115$  and  $0.023 \pm 0.012$ , respectively. These values were much lower than without lubricants. Scanning electron microscopy results confirmed deeper and wilder wear tracks on dry lubricant than those with lubricants. Dry surface exhibited the boundary regime, which the normal load and sliding speed has no influence on its friction regime. By using oil-based lubricant, the friction regime transited from mixed to boundary regime, as the normal load increased. Applying EG-based lubricant, the friction regime transited from mixed for lower sliding speed to hydrodynamic regime for higher sliding speed at 0.1N but transited from mixed regime to boundary regime at 0.5N instead. Moreover, the effects of adding additives in EG based lubricant were also studied. It was found that by added surfactant on EG-based lubricant its friction belongs to boundary regime. While added corrosion inhibitors its friction belongs to mixed regimes.

Department: Physics

Student's Signature .....

Field of Study: Physics

Advisor's Signature .....

Academic Year: 2017

## ACKNOWLEDGEMENTS

My thesis is finally completed after taking a long time. First, I would like to express my deepest gratitude and appreciation to my advisor, Assistant Professor Dr. Sukkaneste Tungasamita, who gave me valuable suggestions all the time of research and study, enlightened and explained the theoretical and related knowledges for my better understanding, helped me with thesis writing and encouraged me not only in master's life but also other issues in my life as well.

My sincere thankful also go to Western Digital (Thailand) Company Limited, this thesis would not have been possible without the support from the company in term of sample materials and place for doing experiments. Moreover, I am thankful for all helps and suggestions that I got from Western Digital staffs.

Besides above of all, I would like to give my gratitude to the chairman Assistant Professor Dr. Rattachat Mongkolnavin and the members of thesis committee, Assistant Professor Dr. Panadda Dechadilok and Mr. Chakkrit Supavasuthi for taking their time, kindness and useful comments in the research. Especially thanks to Assistant Professor Dr. Panadda Dechadilok for her useful suggestions, her helps in writing thesis and her keen interest in fluid lubricants.

Importantly, I would like to give my gratitude to the members of my family, my dad, my mom, my brother and my aunt. They always encouraged and gave me financially support for the whole study. Finally, I would like to thank to my friends for their cheerful advices throughout my master study.

## CONTENTS

	Page
THAI ABSTRACT .....	iv
ENGLISH ABSTRACT.....	v
ACKNOWLEDGEMENTS.....	vi
CONTENTS.....	vii
LIST OF FIGURES .....	x
LIST OF TABLES .....	xii
LIST OF ABBREVIATIONS.....	xiii
CHAPTER I.....	1
INTRODUCTION .....	1
1.1 Hard Disk Drive Technology.....	1
1.2 Motivation.....	2
1.3 Objectives .....	3
1.4 Literature reviews and Scopes of this thesis.....	3
CHAPTER II.....	5
TRIBOLOGICAL OF LAPPING PROCESS AND POWER LAW.....	5
2.1 Lapping Process.....	5
2.2 Tribology .....	6
2.2.1 Friction .....	6
2.2.2 Wear .....	7
2.2.3 Lubricant .....	7
2.3 Physical Properties of liquid lubricant.....	8
2.3.1 Viscosity .....	9
2.3.2 Surface Tension.....	9
2.4 Power law of model of ice friction .....	9
CHAPTER III .....	12
THE EXPERIMENTAL DETAILS .....	12
3.1 Tools .....	12
3.1.1 Tribometer .....	12

	Page
3.1.2 Scanning electron microscope (SEM) .....	15
3.1 Materials .....	16
3.2.1 Solid Materials .....	16
3.2.2 Lubricants .....	16
3.3 Methodology.....	18
3.3.1 Tribological measurement conditions .....	18
3.3.2 Data calculation and Analysis .....	19
CHAPTER IV .....	20
RESULTS AND DISCUSSIONS.....	20
4.1 Effects of dry surface, EG-based and oil-based lubricants on the friction force.....	20
4.1.1 Influences of the normal force exerted on the sliding ball .....	20
4.1.2 Influences of the sliding speed .....	22
4.1.3 Characterization on the tested AlTiC surfaces using SEM .....	25
4.2 Effects of additives in an EG-based lubricant on the friction regime.....	26
4.2.1 Effects of surfactants in the EG-based lubricants on the friction force....	26
4.2.2 Effects of corrosion inhibitor in the EG-based lubricants on the friction force.....	28
4.2.3 Effect of a combination of surfactants and corrosion inhibitors in an EG-based lubricant on the occurred friction. ....	28
CHAPTER V .....	30
CONCLUSIONS AND SUGGESTIONS.....	30
REFERENCES .....	32
VITA.....	36



## LIST OF FIGURES

<b>Fig. 1.1</b> A schematic drawing of hard disk drive [1] .....	1
<b>Fig. 1.2</b> A schematic drawing of head gamble assembly [1].....	2
<b>Fig. 2.1</b> A schematic drawing of lapping process where 1 - 6 are diamond particles [4]. .....	5
<b>Fig. 2.2</b> The diagram of contacting interface (a) macroscopic view and (b) microscopic view [1].....	6
<b>Fig. 2.3</b> A plot of Stribeck curve of journal bearings where $\mu$ is the coefficient of friction, $\eta$ is dynamic viscosity, $\omega$ is angular speed and P is the average pressure carrying load per unit area [15].....	8
<b>Fig. 3.1</b> A schematic of ball-on-disk tribometer [19] .....	13
<b>Fig. 3.2</b> The pictures of components in tribometer: (A) is a DFM-0.5 2D sensor, (B) is a S25UE rotational motor drive, (C) is a suspension and (D) is a ball holder held by suspension .....	14
<b>Fig. 3.3</b> The diagram of electrons generated from a sample when an electron beam interacts with a sample surface .....	15
<b>Fig. 3.4</b> Pictures of materials that were used in the tribological test: (a) the SUS304 stainless steel ball and (b) the Al <sub>2</sub> O <sub>3</sub> -TiC disk .....	16
<b>Fig. 4.1</b> Graphs plot of friction characteristics of SUS304 ball sliding against AlTiC disk with (a) dry surface, (b) EG-based and (c) oil-based lubricants, respectively .....	21
<b>Fig. 4.2</b> A graph plot of friction behavior of SUS304ball sliding against AlTiC disk at various sliding speed in dry, EG- and oil-based lubricants .....	22
<b>Fig. 4.3</b> Graphs log-scale plot between averaged COF and sliding speed of experiments (a) under a dry condition, (b) using an EG-based lubricant and (c) using oil-based lubricant .....	24
<b>Fig. 4.4</b> Electron micrographs of AlTiC surface after tribological measurements under surface condition and force of (a) dry surface at 0.1 N, (b) dry surface at 0.5 N, (c) lubricated with EG-based lube at 0.1 N, (d) lubricated with EG-based lube at 0.5 N, (e) lubricated with oil-based lube at 0.1 N, and (f) lubricated with oil-based lube at 0.5 N. Note that all the samples were from the sliding speed of 3600 mm/min. ....	25

**Fig. 4.5** Graph log-scale plot of EG- and surfactant-modified lubricants on AlTiC disk sliding against SUS304 ball at 0.5N with various sliding speed.....27

**Fig. 4.6** Electron micrographs of wears on AlTiC surfaces after tribology measurement with surfactant (a) PO, (b) QA and (c) PEAL modified lubricants .....27

**Fig. 4.7** Graph log-scale plot between sliding speed and average COF of EG-based lubricant mixed with corrosion inhibitor .....28

**Fig. 4.8** Graph log-scale plot between sliding speed and average COF of EG based lubricant with both corrosion inhibitor and surfactant.....29



## LIST OF TABLES

<b>Table 3.1:</b> Tribology test modes.....	13
<b>Table 3.2:</b> Physical properties of all lubricants .....	17



## LIST OF ABBREVIATIONS

AlTiC	Aluminum titanium carbide
$\omega$	Angular speed
cP	Centipoise
COF( $\mu$ )	Coefficient of friction
$Q_p$	Conducted heat
$\rho_p$	Density
$\eta$	Dynamic viscosity
$F_x$	Friction force
$Q_f$	Frictional heat
HDD	Hard disk drive
h	Lubricant thickness
min	Minute
mL	Milliliter
mm	Millimeter
ns/cm	Nano siemens/centimeter
nm	Nanometer
N	Newton
$F_N$	Normal load force
% wt.	Percent by weight
rpm	Round per minute
SEM	Scanning electron microscope
$R_a$	Surface roughness
$\lambda_p$	Thermal conductivity

## CHAPTER I

### INTRODUCTION

#### 1.1 Hard Disk Drive Technology

Hard disk drive (HDD) is another important part of computer for data and operating system storage by using writing and reading magnetic bits of the binary information. Normally, HDD consists of slider/head, media platter and actuator arm, motor and circuits, as shown in Fig.1.1. During HDD operation, the media disk is rotated at a very high speed and the reader/writer head which is stitched on suspension at actuator arm will be loaded on the disk. If the HDD does not in use, the slider on suspension is pulled back from the disk to the load/unload.

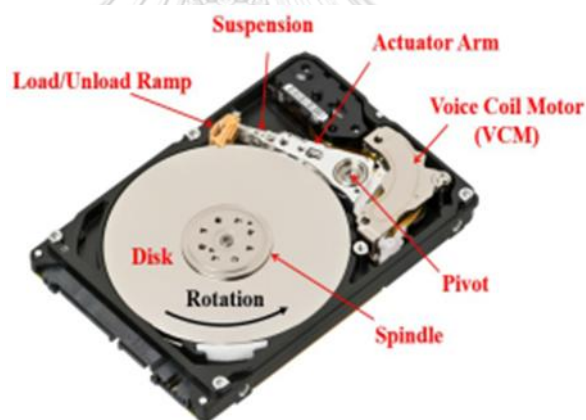


**Fig. 1.1** A schematic drawing of hard disk drive [1]

Fig.1.2 shows a schematic of head gamble assembly (HGA). One of the important parts is a slider. Slider/head is a small important part moving above the media platter and transform the platter's magnetic field into an electrical current (during the disk reading) or transform an electrical current into a magnetic field (in the process of disk writing) during data access operation. The slider consists of many layers of thin film materials which were grown in a well-designed layer on an Aluminum titanium carbide ( $\text{Al}_2\text{O}_3\text{-TiC}$ ) substrate. These layers create the magnetic signal during read/write data on the disk. As the slider flies over the media disk during the operation, the gap between them is extremely small, at only 7-9 nanometers, in order to receive and transfer magnetic signal. The air bearing surface (ABS) underneath the slider with its specific design etched surface helps to provide the pressure contribution to keep a constant space between the slider and the disk during the HDD operation [1].

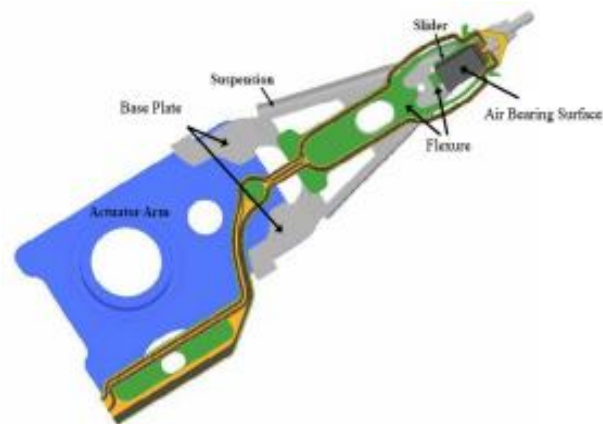


**Fig. 1.2** A schematic drawing of head gimble assembly [1]

For many years, the data reading was completed through an inductive sensing of the magnetic fields associated with the magnetic transition in the medium. In 1990, IBM introduced a magnetoresistive sensor [2]. Since the amplitude of the read back signal is proportional to the width of the recording track, introducing the more sensitive magnetoresistive transducer means reducing the track width and thereby, increasing the track density. The initial magnetoresistive sensors employed perm alloy, an alloy of Ni and Fe, which has a magnetoresistance of 2%; there is a 2% change in the resistance when the magnetization changes from being aligned with the current to being perpendicular to it. This is referred to as the anisotropic magnetoresistive effect [3].

In the near future, the data capacity of 1 TBit/in<sup>2</sup> areal densities will be the next goal of achievement. The electrical, mechanical and magnetic properties and the performance of the slider head have a significant role for the HDD system performance in term of speed and reliability. Those kinds of performance depend strongly on the quality of each stacked layer of materials in the slider structure and the finishing surface of the slider before assembly into HDD [4].

## 1.2 Motivation

For HDD slider fabrication process, the smoothness surface without any defect is the 1<sup>st</sup> priority requirement, in order to achieve the higher recording densities and small flying height. Therefore, surface finishing quality of the recording head or slider is one of the important keys for improving performance of HDD [4]. To get a smooth surface, lapping processes in the slider fabrication process line is important. Lapping process is a process in which two surfaces are rubbed in order to remove thin film layers material on slider and get rid of surface roughness [5]. There are many factors to be considered in the lapping process such as lapping plate, the size of diamond particles and the

properties of lubricants. During the contact of two surfaces, a friction force is generated, and the material removal mechanism starts. Adding lubricant into the system is not only reducing the unnecessary friction force but can also help transferring heat and debris away. This prevents the surface defect formation, such as smear to occur. Some modified lubricants can also function as a corrosion protection. It can be said that lubricant is one of the important parameters in the lapping process. Fundamental knowledge of Tribology, which is the study that focuses on friction, wear and lubrication, can be described as the relationship between parameters in lapping process.

Tribological parameters in the lapping process include the normal force exerted on the slider, sliding speed of lapping plate and type of the lubricant. If the physical properties of lubricant changes, it can affect other parameters. There is also a time-cost-performance effectiveness bonus to select a suitable lubricant, based on their tribological characteristics before applying in the actual fabrication.

### 1.3 Objectives

The objectives of this thesis are

1. To understand the effects of physical parameters including sliding speed, lubricant viscosity and loaded pressure on friction force exerted on the AlTiC disk during the contact between the AlTiC disk, the lubricant and the SUS304 stainless steel ball by using a ball-on-disk tribometer.
2. To investigate the effect of additive additions in lubricants on these tribological parameters.

### 1.4 Literature reviews and Scopes of this thesis

The study in this field has been done for decades. Example of previous experimental works that employed the ball-on-disk tribometer in the determination of tribological parameters include the work of Lui and Deng [6] where the friction originated from having a silicon carbide ball (with coating of TiN, TiAlN and CrAlN) sliding on a tungsten carbide disk in absence of the lubricant was investigated with an aim of studying the wear resistance. Their results showed that the coefficient of friction (COF) was smaller if the ball was TiN and TiAlN than that obtained from the ball coated with CrAlN. Fei and Yuan [7] studied the effect of different types of lubricant on the friction originated from having an Al<sub>2</sub>O<sub>3</sub> coated surface sliding against a silicon nitride ball (Si<sub>3</sub>N<sub>4</sub>). The lubricants were water, oil and dry and the obtained friction coefficient was compared. They found that with increasing applied normal load and speed, the coefficient of friction decreased in oil and water whereas dropped in dry. The friction regime on oil seemed to be hydrodynamic which it can carry load and absorb the friction force. Moreover, the mechanisms of wear were found to be different if different lubricants were employed. For dry friction, the observed wear on the disk surface was

the abrasive wear, whereas micro-ploughing wear was found on the disk surface when the lubricant was oil. When water was employed as a lubricant, both types of wear were observed. Moreover, there is a study that has been done on another type of tribometer. Ding and Dai [8] studied the friction and wear during the sliding contact of titanium disk and carbon ball in water and artificial sea lubricant. It was found that COF decreases with increasing normal load and frequency. More numbers of wear were observed when the experiment was conducted in the artificial sea than that observed when it was conducted in water.

In this thesis, the ball-on-disk tribometer was employed in order to investigate the effects of Ethylene Glycol (EG) based lubricant and the oil-based lubricant on COF during the lapping process.





## CHAPTER II

### TRIBOLOGICAL OF LAPPING PROCESS AND POWER LAW

#### 2.1 Lapping Process

Lapping process is alike polishing process that a high quality, fine surface finishing with high dimensional accuracy are needed, especially in microelectronic manufacturing. The mechanism of lapping process is carried to flat surface. Generally, there are three components involved in the lapping process. The first component is the lap plate which is embedded or charged with diamond or hard particles in order to remove another material in the sliding contact motion. During operation, the lap plate is rotated with adjustable rotational speed. The second component is called a work piece; the material of the work piece will be polished during the process. The last component is the lapping fluid, a lubricant that is added during the lapping process and flows between the lapping plate and the work piece in order to reduce friction and transfer heat away from their interface [4]. Moreover, some modified lubricant has a special function to capture the wear debris or prevent the corrosion on any specific material surface. The schematic of lapping process is shown in Fig. 2.1.

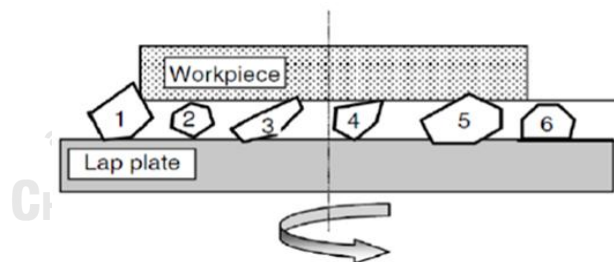


**Fig. 2.1** A schematic drawing of lapping process where 1 - 6 are diamond particles [4].

There are many important factors influencing the lapping process. The main factors are the tribological factors, such as normal force applied on the work piece ( $F_N$ ), rotational velocity of the lap plate, the grain size of diamond particle and the viscosity of the lubricant. These tribological factors play a very significant role in the real processes.

## 2.2 Tribology

Tribology is defined as the science of interacting surface in relative motion [9], [10]. The word “tribos” comes from Greek which means rubbing [11]. As mentioning earlier in the previous chapter, tribology focuses on the study of friction, wear and lubrication. Amontons first proposed the equation of friction force in 1699. He explained that friction force, ( $F_X$ ) between two bodies in sliding contact is a proportional of normal load force, ( $F_N$ ) and coefficient of friction, ( $\mu$ )[12].

$$F_X = \mu F_N \quad (2.1)$$

Friction is a main cause of wear and material loss. Wear affects the lifetime of machine parts. To reduce friction and wear, lubricant is applied. In modern industry, tribology has a significant role because there are many processes that uses relative surface motion including the lapping process. The roles of those 3 components in tribology will be described in the next part.

### 2.2.1 Friction

Friction is defined as the resistance to motion during sliding of two surfaces in contact. It can be observed as friction heat generation, noise or vibration [11]. There are two types of friction which can be referred to dry friction and friction with lubrication. Dry friction is a resistance to motion of two dry surfaces while lubricated friction is influenced by the fluid viscosity and solid-liquid interaction. Normally, friction occurred during surface contact can be considered both in macroscopic and microscopic views as shown in Fig. 2.2 (a) and 2.2 (b).

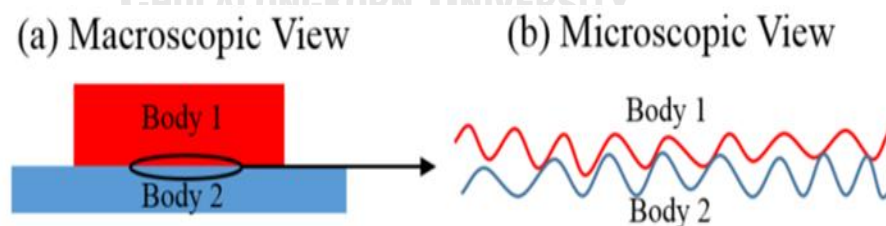


**Fig. 2.2** The diagram of contacting interface (a) macroscopic view and (b) microscopic view [1]

The contact area in macroscopic view is called apparent contact areas. Microscopically, however, only some asperities are touching and overlaps of asperities can generate either elastic or plastic deformation, contributing to the occurrence of

friction force [1]. When hard asperities slide against soft asperities, the material of soft asperities can be worn out, increasing the friction force.

Although, theoretically, Coulomb's law proposed that the friction force and COF are independent of the sliding velocity, many research groups found that the friction force will not remain stable when there is a change in the sliding velocity [7], [11]. On the other hand, the friction force can be generated in a form of oscillation referred to a stick-slip phenomenon. The friction force is quite complicated. It depends on both the materials that are in contact as well as the operating conditions such as sliding velocity and exerted normal force [13].

### 2.2.2 Wear

The definition of wear is the material loss due to contacting surface being in a relative motion [14]. There are several types of wear as follows:

- Abrasive wear occurs when two surfaces with different hardness are in contact. The hard asperities penetrate the softer asperities and causes material removal. In this case, the lubricant can be helped washing the wear particles out of the interface.
- Adhesive wear is generated by adhesive force between two contacting surfaces when there is a bond between two contacting surfaces. If the bond is broken, then the material on the surface with low cohesive energy will be removed.
- Fatigue wear is caused by a damage of material as a result of repeatedly exerted force. Crack or holes are often found on the surface.
- Corrosive wear is a material removal due to chemical reaction. In this case, lubricant can help in two ways by being surface coating to prevent oxidation and capturing the wear debris away from contacting surfaces.

### 2.2.3 Lubricant

Many fluids are commonly employed as lubricants with an aim of reducing friction and wear on surfaces of the polished materials. The lubricant can be liquid, solid or gas [14]. A change in lubricant thickness relative to surface roughness,  $h/R_a$ , during the sliding contact is found to cause a change in relationships between the friction force exerted on the surfaces and physical parameters of the systems. These different dependences are often categorized as different "friction regimes". Shown below in Fig. 2.3 is the Stribeck curve, where three different friction regimes are introduced: boundary friction, mixed friction and hydrodynamic friction [15]. Boundary friction describes the sliding contact of two surfaces (with lubricant in between) in the limit of  $h/R_a \rightarrow 0$ , where the friction coefficient  $\mu$  is found to be independent of  $\eta\omega/P$  where  $\eta$

is the lubricant viscosity,  $\omega$  is the plate angular speed and  $P$  is the applied loaded pressure. In contrast, hydrodynamic friction occurs when the lubricant thickness is larger than the surface roughness ( $h/R_a \gg 1$ ). An increase in the shear stress between surfaces leads to a higher friction coefficient;  $\mu$  is found to increase as a function of  $\eta\omega/P$ . The mixed regime is characterized as the transition state between the boundary and hydrodynamic friction regimes where  $h/R_a \sim 1$  (the lubricant thickness is comparable to the surface roughness). In this regime,  $\mu$  is found to decrease as a function of  $\eta\omega/P$ .

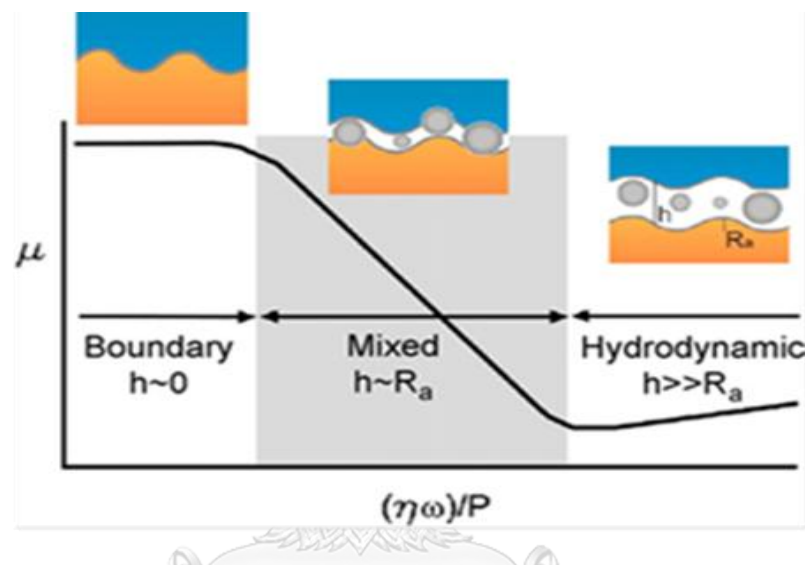


**Fig. 2.3** A plot of Stribeck curve of journal bearings where  $\mu$  is the coefficient of friction,  $\eta$  is dynamic viscosity,  $\omega$  is angular speed and  $P$  is the average pressure carrying load per unit area [15]

### 2.3 Physical Properties of liquid lubricant

In fact, the main function of lubricant is to reduce wear and friction. It is necessary to verify its properties. In many industry, oil lubricant is commonly used while some process is required another type of liquid lubricant, e.g. water-based lubricant. To select suitable lubricant to the application, the better understand of lubricant physical properties is very important.

### 2.3.1 Viscosity

The parameter that plays significant role is viscosity. It can be defined as the resistance by shear stress. In simple term, viscosity means friction between the molecules of fluid [16]. Viscosity is sensitive and is affected by the change of temperature and heat dissipation of lubricated contact. It can be measured by viscometer. There are 3 types of viscometer; falling viscometer, capillary viscometer and rotational viscometer [13].

### 2.3.2 Surface Tension

Surface tension is the cohesive force between liquid molecular. Various lubricants show differences of degree of wetting and spreading. Moreover, some additives can be added to reduce surface tension of lubricant [10].

### 2.4 Power law of model of ice friction

There have been several theoretical attempts to investigate the relationship between the frictional force exerted on the surfaces and the physical properties of the slider, the plane and the lubricant in the context of ice friction, which the frictional force is viewed as heat generated per unit displacement [17]. According to the further elaborated model of Oksanen and Keinonen [18], the frictional heat,  $Q_f$  can be generated during a time interval  $b/v$  (where  $v$  is the sliding speed and  $b$  is the dimension of the slider in the same direction as the sliding velocity) As two surfaces ( $S_P$  and  $S_S$ ) are in sliding contact with liquid lubricant contained between surfaces, the  $Q_f$  can be written as equation shown below.

$$Q_f = \mu F_N v \left( \frac{b}{v} \right) \quad (2.2)$$

$F_N$  is the loaded normal force. The amount of heat conducted into the surface  $S_P$  during the time interval  $b/v$  is

$$Q_P = \frac{\lambda_P A \Delta T_P}{\delta} \left( \frac{b}{v} \right) \quad (2.3)$$

where  $Q_P$  is the conducted heat during this time interval.  $\lambda_P$  and  $\Delta T_P$  are the thermal conductivity of the surface  $S_P$  and the temperature difference between the contact

surface and the bulk solid, respectively.  $A$  is the contact area, whereas  $\delta$  is the thickness of the solid slab into which the heat is conducted.  $Q_P$  is equal to the energy required in raising the temperature in the heat layer, which can be estimated as follows.

$$Q_P = \rho_P A \delta c_P \frac{\Delta T_P}{2} \quad (2.4)$$

where  $\rho_P$  is the density of the solid, and  $c_P$  is its specific heat capacity. Equating Eqs. (2.3) and (2.4), the unknown parameter  $\delta$  can be eliminated. Then,  $Q_P$  can be expressed as

$$Q_P = A \Delta T_P \left( \frac{b}{2v} \right)^{1/2} (\lambda_P c_P \rho_P)^{1/2} \quad (2.5)$$

Using the same expression for the heat conducted into the surface  $S_s$  ( $Q_s$ ), the total heat conducted into the two surfaces can be found as follows.

$$Q_P + Q_s = A \Delta T_P \left( \frac{b}{2v} \right)^{1/2} (\lambda_P c_P \rho_P)^{1/2} + A \Delta T_s \left( \frac{b}{2v} \right)^{1/2} (\lambda_s c_s \rho_s)^{1/2} \quad (2.6)$$

The heat required in raising the temperature of the lubricating layer during the contact in the time interval  $b/v$  is as shown below.

$$Q_L = Ah \rho_L c_L \Delta T_L \quad (2.7)$$

where  $h$  is the lubricating layer thickness.  $\rho_L$  and  $c_L$  is the density and the specific heat capacity of the lubricant, whereas  $\Delta T_L$  is the lubricant temperature increase during the time interval  $b/v$ .

Under the assumption that the friction heat generated ( $Q_f$ ) equals to the heat conducted into the two surfaces and the heat required in raising the temperature of the lubricating layer ( $Q_P + Q_s + Q_L$ ) during the same time interval, we can obtain:

$$\begin{aligned} \mu F_N v \left( \frac{b}{v} \right) &= A \Delta T_P \left( \frac{b}{2v} \right)^{1/2} (\lambda_P c_P \rho_P)^{1/2} + A \Delta T_s \left( \frac{b}{2v} \right)^{1/2} (\lambda_s c_s \rho_s)^{1/2} \\ &+ Ah \rho_L c_L \Delta T_L \end{aligned} \quad (2.8)$$

From Eq. (2.8), it can be deduced that the lubricant layer thickness ( $h$ ) is as follows.

$$h = \frac{1}{c_L \rho_L \Delta T_L} \left( \begin{array}{l} \frac{\mu F_N b}{A} - \Delta T_P \left( \frac{b}{2v} \right)^{1/2} (\lambda_P c_P \rho_P)^{1/2} \\ - \Delta T_S \left( \frac{b}{2v} \right)^{1/2} (\lambda_S c_S \rho_S)^{1/2} \end{array} \right) \quad (2.9)$$

Based on the assumption that the lubricating layer is the main source of frictional resistance, the frictional force can be expressed as the product of the shear stress exerted onto the surface and the contact area as follows.

$$\mu F_N = \eta \left( \frac{v}{h} \right) A \quad (2.10)$$

Substituting the expression for  $h$  from Eq. (2.9) into Eq. (2.10), a quadratic equation is obtained as shown below.

$$\mu^2 \left( \frac{F_N^2 b}{A} \right) - \left( \frac{b}{2v} \right)^{1/2} \left[ \Delta T_P (\lambda_P c_P \rho_P)^{1/2} + \Delta T_S (\lambda_S c_S \rho_S)^{1/2} \right] \mu F_N - \eta v A c_L \Delta T_L = 0 \quad (2.11)$$

A solution of Eq. (2.11) is simply.

$$\mu = \frac{1}{2} \frac{A}{F_N b} \left( \frac{b}{2v} \right)^{1/2} \left\{ \Delta T_P (\lambda_P c_P \rho_P)^{1/2} + \Delta T_S (\lambda_S c_S \rho_S)^{1/2} \right\} \pm \left[ \frac{A^2}{8 F_N^2 b} \left( \frac{1}{v} \right) \left\{ \Delta T_P (\lambda_P c_P \rho_P)^{1/2} + \Delta T_S (\lambda_S c_S \rho_S)^{1/2} \right\}^2 + \frac{\eta v A c_L \Delta T_L \rho_L A}{F_N^2 b} \right]^{1/2} \quad (2.12)$$

From Eq. (2.12) for small lubricant thickness, it relates to surface roughness and corresponds to the mixed friction regime, where  $\mu$  declines as a function of sliding speed  $\mu \propto v^{-1/2}$ . For large lubricant thickness, it relates to surface roughness and  $\mu$  increases as a function of sliding speed  $\mu \propto v^{+1/2}$ . This dependency is observed in the occurrence of the hydrodynamic friction, where the small roughness of surface leads to a higher shear stress between the two surfaces.

In this study, we have investigated the relationship between  $\mu$  and sliding speed, in order to determine the friction regime. The effects of the lubricant viscosity and the applied normal force  $F_Z$  on the coefficient of friction were also examined [18].

## CHAPTER III

### THE EXPERIMENTAL DETAILS

This chapter contains three main parts which are Tools, Materials and Methodology, that have been used in this thesis.

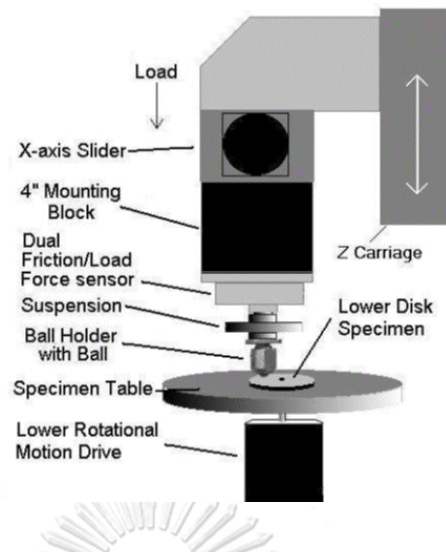
#### 3.1 Tools

The characterization equipment that have been used in thesis for surface/lubricants analysis are described in this section.

##### 3.1.1 Tribometer

The BRUKER CETR UMT-2 micro-tribometer with a ball-on-disk configuration was used as the main tools to characterize the tribological property of the lubricants. There are 2 main hardware parts for this tribometer; upper specimen and lower specimen. At the upper specimen, the ball shape probe which is held up by ball holder is slide against the rotational disk. There are two-dimensional (2D) force sensors that use for measuring the sliding friction force between the upper and lower specimen and the loaded force controlling. In order to remains constant loading force, suspension has been used with the system. Suspension is a spring device used for compensating for variation in the distance between the force sensors and the surface of disk during motion. Moreover, there are the vertical carriage stage and lateral positioning stage. The vertical carriage stage is a driven motor for encoding position feedback. It provides the upper loading force pressing on lower disk specimen and the lateral positioning stage is used to offset the upper specimen from center axis. It can be set the radius at which ball touches disk [19]. For lower specimen hardware part, it consists of a disk holder and rotational motor drive. The speed of rotational motor can be programed. The configuration of CETR UMT-2 microtribometer in ball-on-disk is shown in Fig. 3.1 [19].

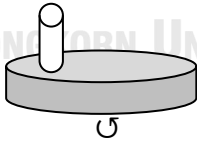
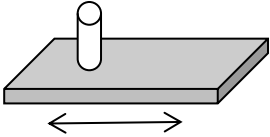
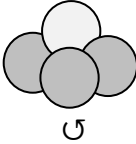


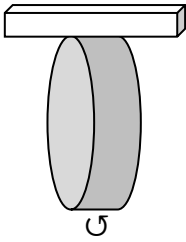
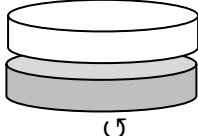


**Fig. 3.1** A schematic of ball-on-disk tribometer [19]

There are several tribometer test modes such as pin-on-disk, ball-on-disk or block-on-ring tribometer as shown in Table 3.1 [20].

**Table 3.1:** Tribology test modes

Typical tribology test modes	Model	Description
ball/pin-on-disk		Sliding wear and friction behavior between a static pin or ball and a rotating surface
ball/pin-on-plate		Sliding wear and friction behavior between a static pin or ball and a linear displacing surface
4-ball		High pressure lubricant/grease characterization test

block-on-ring		Sliding wear and friction behavior between a block and a radial ring
disk/ring-on-disk		Sliding and/or rolling wear and friction behavior two disk or ring surfaces sharing the same axes

In this thesis, the initial contact was a point contact sliding against the rotational motion disk. The disk was mounted on a lower rotational drive and the ball was mounted on upper specimen. During, the measurement, the force load is applied vertically downward with a motor driven carriage that uses the force/load sensor for feedback to remain a constant load. The coefficient of friction (COF) is then calculated by the software program using the load force and friction force values.

The model of 2D force sensors is called DMF-0.5 which it provides the range of 0.05 to 5 N and it can be measured precisely with the resolution of 0.00003% of full scale. The model of rotational motor drive is the S25UE-0195A. It can be adjusted the speed from the range of 0.001 to 5000 RPM and accepted the load maximum of 5N. In addition, the choices of suspension and size of ball holder should match the sensitivity of force sensor. In this tribometer, the ball holder size is 3.302 shaft. These components are shown in the Fig 3.2.



**Fig. 3.2** The pictures of components in tribometer: (A) is a DMF-0.5 2D sensor, (B) is a S25UE rotational motor drive, (C) is a suspension and (D) is a ball holder held by suspension

### 3.1.2 Scanning electron microscope (SEM)

Scanning electron microscope (SEM) is a useful technique to observe and inspect the surface morphology or microstructure of samples. JEOL JSM-6480LV scanning electron microscope was used in this thesis. The components of SEM consist of electron gun, vacuum chamber, condenser lens, deflection coil, camera and detectors. Electrons are produced at electron gun and travel through the vacuum chamber to prevent collision of electron in air. The electromagnetic condenser lens condenses electrons into a beam and focuses the beam on the sample surface. The electron beam can be adjusted to the whole surface. The interaction of the electrons in SEM results in different phenomena, as shown in Fig. 3.3. As the electron beam incident on the surface, different types of electrons are reflected and detected by the detectors such as secondary electron (SE), back-scattered electron (BSE), Auger electron and photons [21].

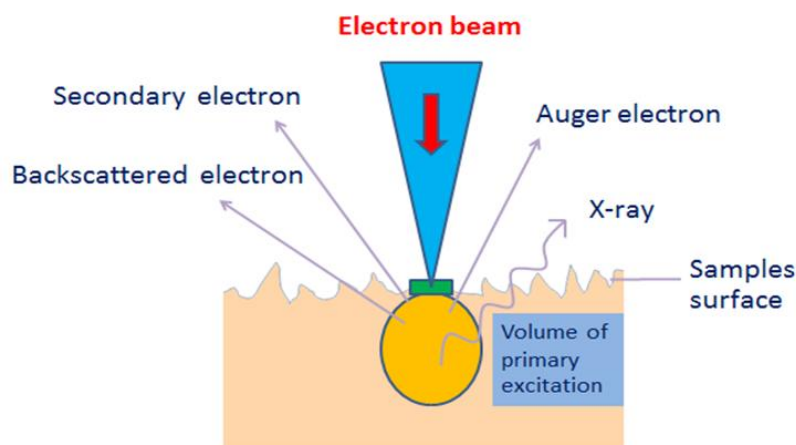


**Fig 3.3** The diagram of electrons generated from a sample when an electron beam interacts with a sample surface

SEM provides white and back contrast due to the amount of secondary or back scattered electrons detected. If incident electrons are directed into valley area, the numbers of detected secondary electron will be small then the dark area will appear. In the other hands, if incident electrons are directed into peak area, enormous number of secondary electrons will be detected and bright area occurs [21].

### 3.1 Materials

#### 3.2.1 Solid Materials

For trio-pair testing via ball-on-disk tribometer, the SUS304 stainless steel balls with a diameter of 6.35mm were used as ball probe. Aluminum titanium carbide ( $\text{Al}_2\text{O}_3\text{-TiC}$  as known as AlTiC) disk with a diameter of 76.23mm was used for disk counterpart. This AlTiC surface hardness was about 2000 HV and had the surface roughness at  $0.0104\ \mu\text{m}$ , as shown in Fig 3.4.

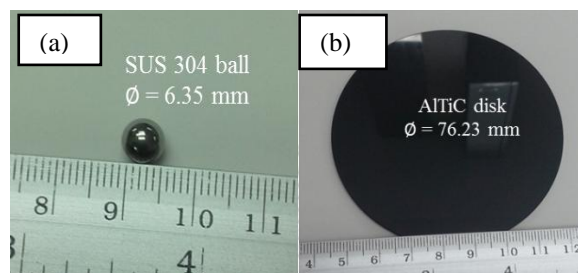


**Fig. 3.4** Pictures of materials that were used in the tribological test: (a) the SUS304 stainless steel ball and (b) the  $\text{Al}_2\text{O}_3\text{-TiC}$  disk

#### 3.2.2 Lubricants

Generally, ethylene glycol (EG) based lubricant is used in final lapping process of HDD read-write head (slider) production. Due to the changes of some thin film layers in the slider, the oxidation and corrosion were occurred and caused failure in the production. The modified-EG lubricant, with functional additives and the oil-based lubricant are now in focus. In this thesis, we have investigated on the fundamental effects of different lubricant on their tribological parameters. The experimental results were compared between dry (no lubricant), EG-based and oil-based lubricants, to understand the common behaviors of each type of lubricant during the sliding/lapping motion. Later, the effects from the additional additives in EG were also measured. Table 3.2 shows the basic properties of all lubricants that were used in this thesis.

**Table 3.2:** Physical properties of all lubricants

Properties	Lubricants								
	EG	EG + surfactants			EG + corrosion inhibitors		EG + combination of surfactant and corrosion inhibitor		Oil
		PO	QA	PEAL	PP	PO	PP+EAO	PO+EAO	
Ethylene glycol (%wt.)	93.126	92.126	92.126	92.126	93.058	93.058	93.058	93.058	-
TEA (%wt.)	6	6	6	6	6	6	6	6	-
BTA (%wt.)	0.011	0.011	0.011	0.011	0.011	0.011	0.011	0.011	
Inhibitor A (%wt.)	0.075	0.075	0.075	0.075	1	1	1	1	0.2
Inhibitor B (%wt.)	0.5	0.5	0.5	0.5	0.15	0.15	0.15	0.15	-
Corrosion Inhibitor PP (%wt.)	-	-	-	-	0.06	-	0.06	-	-
Surfactant /Corrosion Inhibitor PO (%wt.)	-	0.2	-	-	-	0.06	-	0.06	-
Surfactant EAO (%wt.)	-	-	-	-	-	-	0.08	0.08	-
Surfactant QA (%wt.)	-	-	1	-	-	-	-	-	-
Surfactant PEAL (%wt.)	-	-	-	1	-	-	-	-	-
Petroleum Hydrocarbon (%wt.)	-	-	-	-	-	-	-	-	61.75
Conductivity (nS/m)	126.4	113.7	105.7	187.4	117.23	136.03	-	-	225
Viscosity at 25° C (cP)	20	19.0	19.4	19.6	19.05	-	-	-	1.88
pH	8.4	8.5	8.5	8.2	8.55	8.52	-	-	5.39

The chemical names are as followed:

1. Ethylene glycol (Innovative Organics Company)
2. Triethanolamine, TEA (Merck)
3. Benzotriazole, BTA (Innovative Organics Company)
4. Potassium nitrite, Inhibiter A (Innovative Organics Company)
5. 6,6,6-(1,3,5-Triazine-2,4,6-triyltriimino) trihexanoic, Inhibiter B (CHEMOS, 99%)
6. Ethoxylated amine oxide, EAO (Saint Gobain Ceramic Materials)
7. Decaethylene glycol monododecyl, PEAL (Sigma Aldrich)
8. Alkylated amineoxide, AAO, Tomamine AO-14-2 (Air Product industry co. ltd)
9. Quaternary amines, Tomamine, QA, Q-14-2 (Air Product industry co. ltd)
10. Polyoxyethylene- (20) - sorbitanmonostearate, Tween 20, PO (Chemipan Corporation Co., Ltd., Thailand)

### 3.3 Methodology

A ball-on-disk tribometer was used for tribo-test. The contact load was determined by applying weight on ball directly and the friction force was measured by using sensor. The signal from load cell with a sample rate of 10Hz was stored in the computer. The COF values of each measured condition were calculated, compared and analyzed with the power law. The SEM was used to observe the surface of the AlTiC disk after tribo-test for the surface scratching.

#### 3.3.1 Tribological measurement conditions

To understand the tribological characteristics of different contact system (dry surface, surface with EG-based and oil-based lubricants) at different applied loaded force, the applied loaded force of 0.1 and 0.5 N were set. Note that, the pressure with 0.1N is as similar as the pressures in the actual final lapping process. The sliding speed was varied from 300 to 3600mm/min. This condition was as similar as sliding speed in final lapping process. The contact number of cycle was set for 150 rounds and each test was repeated 3 times. Thus, the changes of applied load and sliding speed that can affect on characteristic of surface with different lubricants, were carefully investigated.

Moreover, the functional additives in lubricant such as PO, QA and PEAL were mixed with EG-based lubricant and their COF of each case were extracted and analyzed.

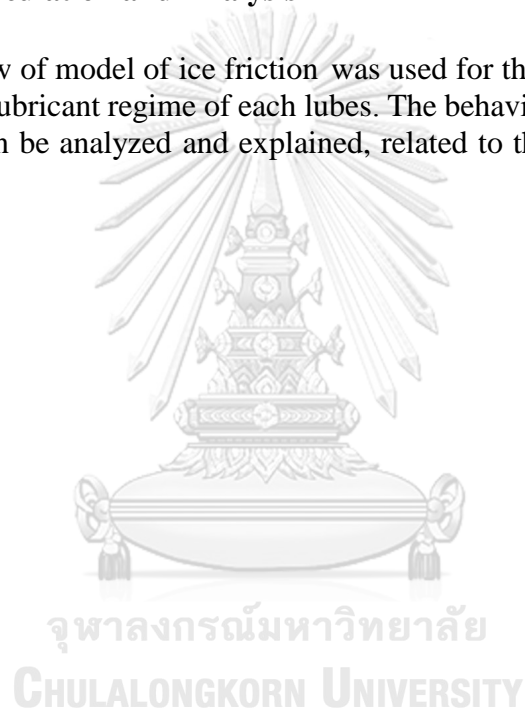
The procedure steps of tribo-test are done as follow:

1. The script-program was inputted into controlling software to set the applied load, sliding speed and radius of contact.
2. 15 ml of lubricant was filled on the AlTiC disk surface.

3. The measurement was done under the configuration that SUS304 ball was fixed and AlTiC disk was rotated in clockwise.
4. Flush out the tested lubricant and refill another 15 ml of lubricant into the system and repeat the measurement for 3 times of each lubricant
5. Clean the ball holder and the disk holder with SC19 and Isopropanol alcohol and blow dry.
6. Change the new pair of AlTiC disk and ball for each new lubricant, then repeat the measurement.

### 3.3.2 Data calculation and Analysis

The power law of model of ice friction was used for the tribology results analysis to investigate the lubricant regime of each lube. The behaviors of each lubricant under motion contact can be analyzed and explained, related to their physical and chemical properties.



## CHAPTER IV

### RESULTS AND DISCUSSIONS

#### 4.1 Effects of dry surface, EG-based and oil-based lubricants on the friction force

To investigate the effects of lubricants on the friction force occurred during the final lapping process, the experiment was completely done by employing a tribometer, consisting of an SUS304 ball sliding on an AlTiC disk. The friction coefficient (COF) values were measured on the lubricated contact between the ball surface and the AlTiC disk, compared to the dry condition. The utilized lubricants were included ethylene-glycol-based (EG-based) lubricant and a petroleum (oil-based) lubricant. Effects of the normal force exerted on the sliding ball and the sliding speed are discussed further below.

##### 4.1.1 Influences of the normal force exerted on the sliding ball

To mimic the first stage of the HDD slider final lapping process, the sliding ball speed was set at 3600 mm/min and the normal force exerted on the sliding ball was set at 0.1 N (corresponding to the same amount of pressure exerted on the sliding bars). To investigate the effects of the normal force on COF value, the normal force was increased to 0.5 N. The change of COF values was measured and presented in Fig. 4.1. Fig 4.1(a), under a dry condition with the normal force at 0.1 N, the measured COF fluctuated during the first 50 cycles and then, became stable at about  $1.276 \pm 0.085$ . As the normal force increased to 0.5 N, the obtained COF was found at about  $0.540 \pm 0.052$  during the first 50 cycles, before sharply increased and remained at  $1.128 \pm 0.052$ . For dry surface sliding, an increasing of the normal force led to a decreasing of the averaged COF at a constant sliding speed of 3600 mm/min. The similar effect was also observed when the EG-based lubricant was employed. As the EG-based lubricant was added onto the surface of AlTiC wafer, at 0.1N load, it is not possible to measure COF during the first 100 contact cycles because of lack of resolution and COF is very small, then COF raised up to an average of  $0.089 \pm 0.115$ . However, The COF fluctuated after 100 cycles. It might be because of wear track thus led to non-uniform surface roughness in each contact cycle. The experiment for investigation occurrence of wear within 100 cycles is needed to confirm this hypothesis. At the normal force of 0.5 N, an average COF for the whole test (150 contact cycles) was found stably at about  $0.065 \pm 0.014$ .



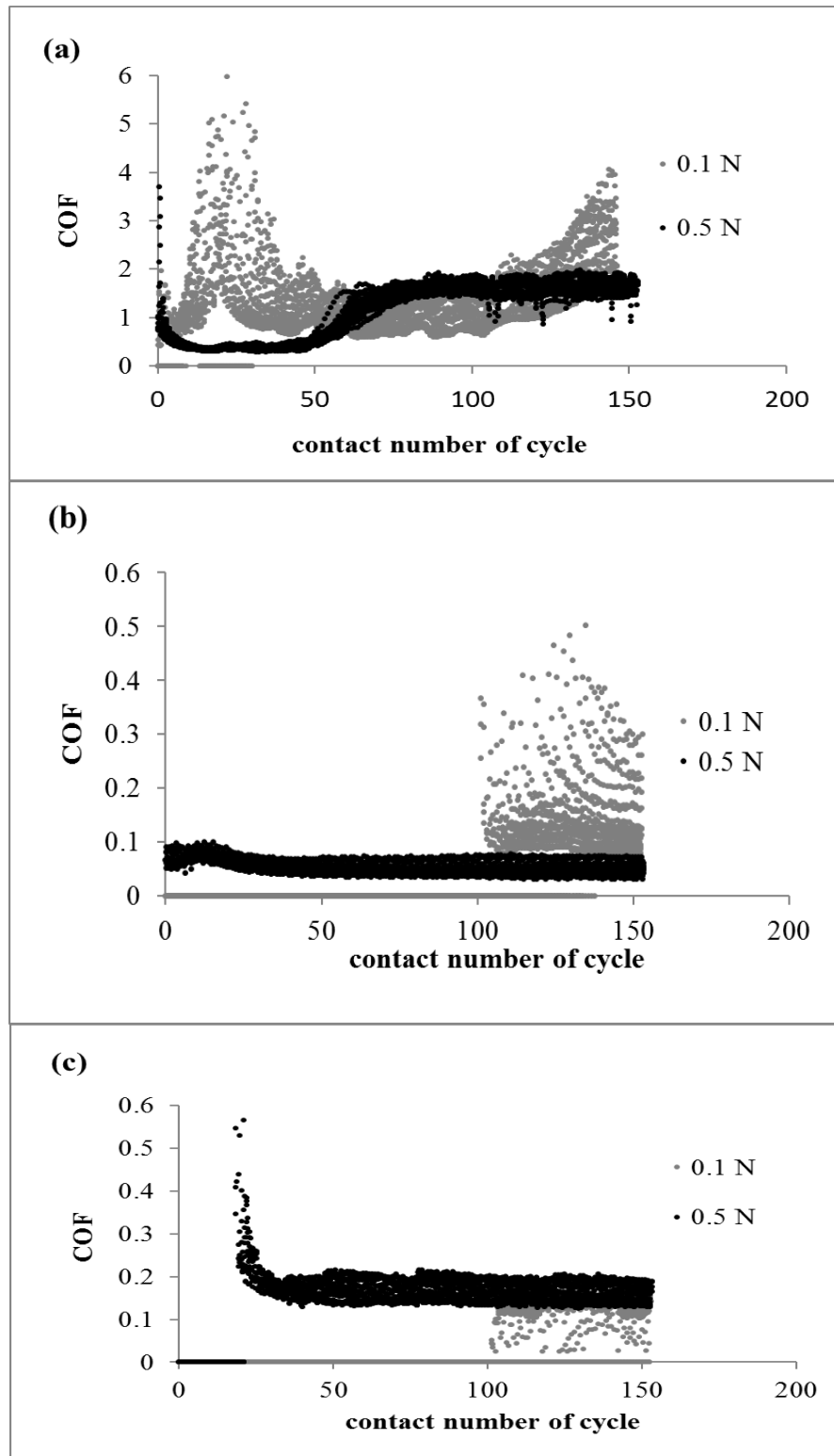


**Fig. 4.1** Graphs plot of friction characteristics of SUS304 ball sliding against AlTiC disk with (a) dry surface, (b) EG-based and (c) oil-based lubricants, respectively

Unlike the behaviors of COF values, obtained from a dry surface condition and a condition that EG-based lubricant covered the surface, an increasing of normal load when using oil-based lubricant, caused an increasing in COF values, as seen in Fig. 4.1(c). The COF of an oil-based lubricant is similar to EG based lubricant during the first 100 contact cycles for force load of 0.1N then it was found an average COF after 100 cycles as  $0.033\pm 0.012$ . For force load 0.5 N, COF remained stable and the average COF was found at about  $0.158\pm 0.007$ . Despite the increase in the COF due to the increase of the normal force, the averaged COF obtained from utilizing the oil-based lubricant was still smaller than those values, obtained from the EG-based lubricant and dry surface cases. To investigate the different effects of the normal force on the friction coefficient when different lubricants are employed and to identify the friction regime, COF was measured as a function of sliding speed as discussed in the next section.

#### 4.1.2 Influences of the sliding speed

In order to investigate the influences of sliding speed on the friction force, the speed of the sliding ball was varied from 3600 mm/min (corresponding to the sliding speed of the sliding bar during the first stage of the final lapping process) to 300 mm/min (the sliding speed in the final stage of the final lapping process) in the measurement. As shown in Fig. 4.2, the effect of the normal force on COF is intertwined with the effect of the sliding speed. For instance, as the EG-based lubricant was placed on the AlTiC surfaces, the COF was decreased as a function of the normal force at the sliding speed of 3600 mm/min but at sliding speed 300 mm/min, the COF increased as the normal forces increased.

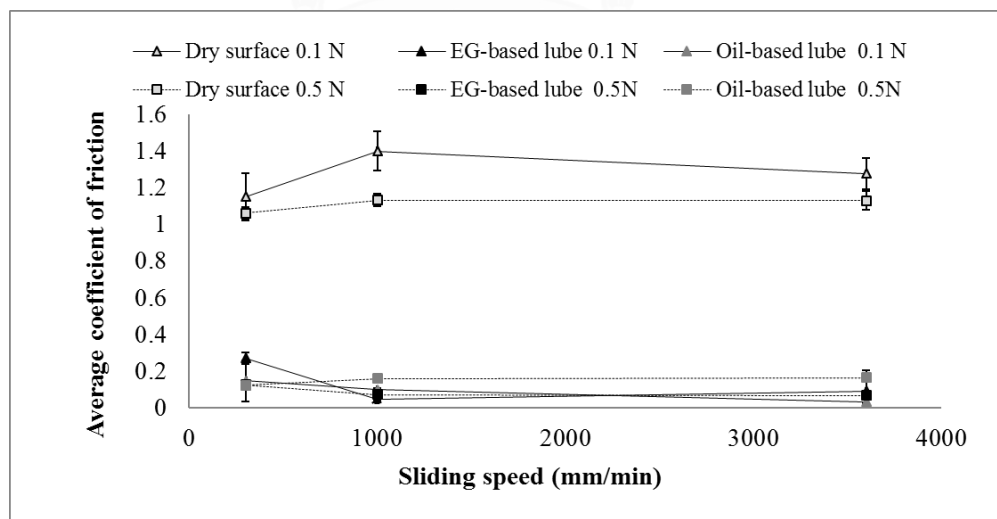


**Fig. 4.2** A graph plot of friction behavior of SUS304ball sliding against AlTiC disk at various sliding speed in dry, EG- and oil-based lubricants

To identify the friction regime, the results in Fig. 4.2 were reported in a logarithmic scale, as shown in Fig. 4.3. According to the Stribeck curve, described in chapter 2, the boundary friction regime, where the lubricant is absent or is present but the lubricant thickness is much less than the surface roughness, can be referred by the fact that the COF is independent from the sliding speed. The mixed regime, where the lubricant thickness is comparable to the surface roughness, is in the case of COF decreases as a function of sliding speed. Whereas, the hydrodynamic regime, where the lubricant thickness is much larger than the surface roughness, corresponds to the regime where COF increases as a function of sliding speed due to an increasing of shear stress between the surfaces [13].

As seen in Fig. 4.3(a), the COF obtained from a dry condition was found to be in the boundary friction regime as expected; the friction coefficient did not change as a function of the sliding speed, at both values of the exerted normal force. From Figs. 4.3(b) and (c), a utilization of a lubricant led to a one-order-of-magnitude reduction of COF value. In addition, as EG-based lubricant was used, the COF became dependent on the sliding speed, implying that the occurred friction belonged to different regimes (see Fig. 4.3(b)). At the normal load force of 0.1 N, the COF decreased as a function of the sliding speed in the beginning and then, increased as a function of the sliding speed ( $v$ ), indicating a possible regime change from the mixed regime to the hydrodynamic regime. A curve-fit of the results on a log-scale indicated that COF decreased as a function of  $v^{-1.518}$  in the beginning and then increased as a function of  $v^{0.5655}$ . The power of 0.5655 was close to the variation as  $v^{1/2}$  of the friction coefficient predicted by Eq. (2.12) as the friction can be referred to the hydrodynamic regime. The increasing speed corresponds to an increase in the shear stress. The initial decline of COF was a function of  $v^{-3/2}$ . However, it was not predicted by the same equation or any other model and further investigation is required [16].

After the normal force exerted on the ball increased to 0.5 N, the COF started to decrease as a function of the increasing sliding speed. COF was varied with  $v^{-0.476}$ . The power of -0.476 was also close to the variation as  $v^{-1/2}$  of the friction coefficient predicted. The friction regime belonged to the mixed friction regime where the lubricant thickness is comparable to the surface roughness. As the sliding speed increased, the measured COF became constant and independent of the sliding speed, indicating a possible transition from the mixed friction regime to the boundary friction regime. This might be due to the decreasing of the lubricant thickness at higher sliding speed, resulting in the lubricant thickness change from being comparable to the surface roughness (the mixed friction regime) to being smaller than the surface roughness (the boundary friction regime) [16].

Fig. 4.3(c) showed the COF values obtained when the oil-based lubricant was employed. With the normal force of 0.1 N, COF monotonically decreased as a function of  $v^{-0.601}$ ; this power relationship is close to the case where COF decreases as  $v^{-1/2}$  in the mixed friction regime. As the normal force was increased to 0.5 N, COF became independent of the sliding speed, indicating that the occurred friction might belong to the boundary friction regime. This might be due to a deeper wear on the AlTiC surface brought about by an increase in the exerted normal force. The observation of the AlTiC surface by scanning electron microscopy (SEM) was performed and discussed in the next section.

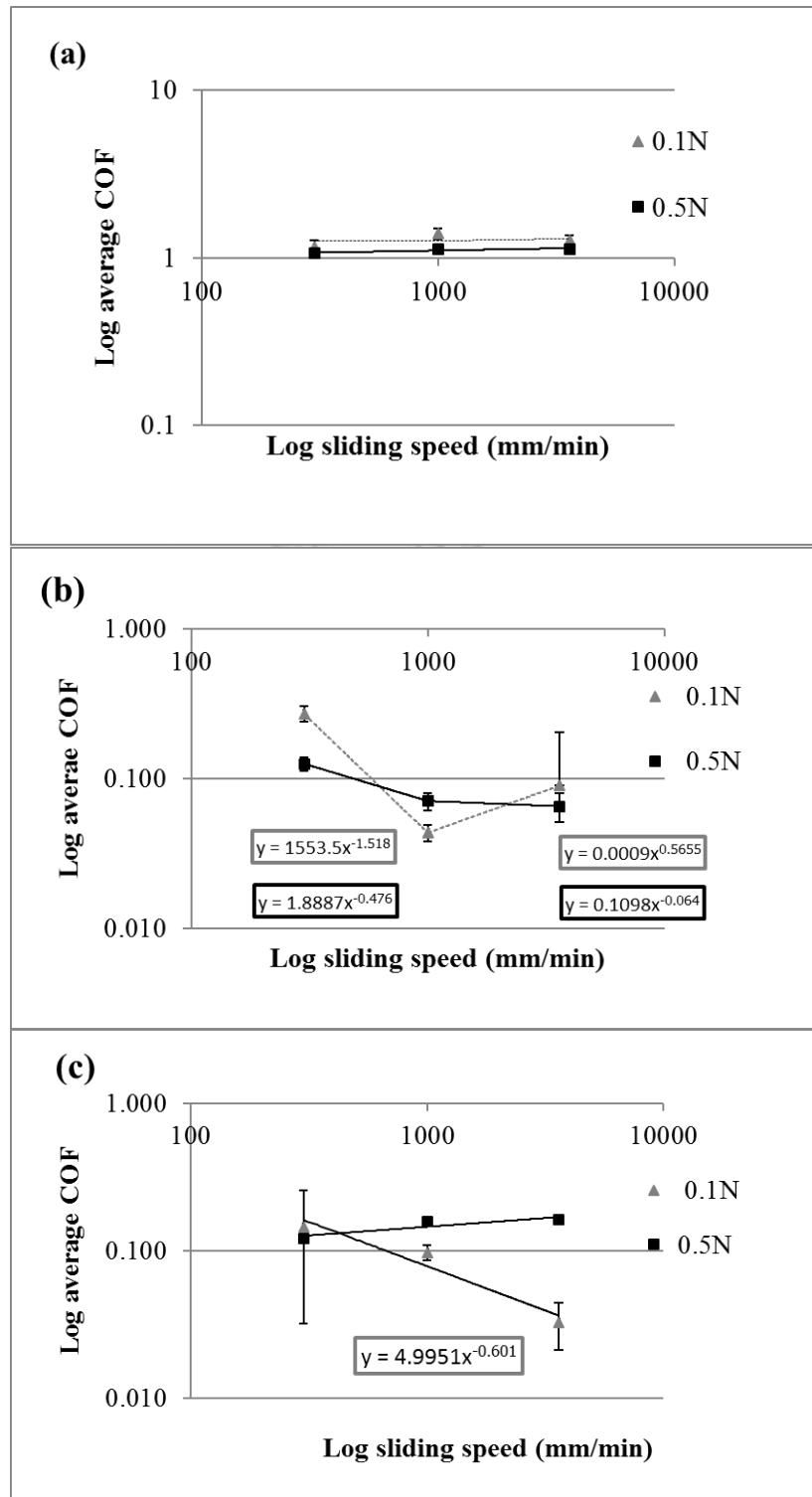


**Fig. 4.3** Graphs log-scale plot between averaged COF and sliding speed of experiments (a) under a dry condition, (b) using an EG-based lubricant and (c) using oil-based lubricant

#### 4.1.3 Characterization on the tested AlTiC surfaces using SEM

Scanning electron micrographs of tested AlTiC surfaces, after the ball-on-disk measurements by tribometer with sliding speed at 3600 mm/min, were presented in Fig. 4.4.

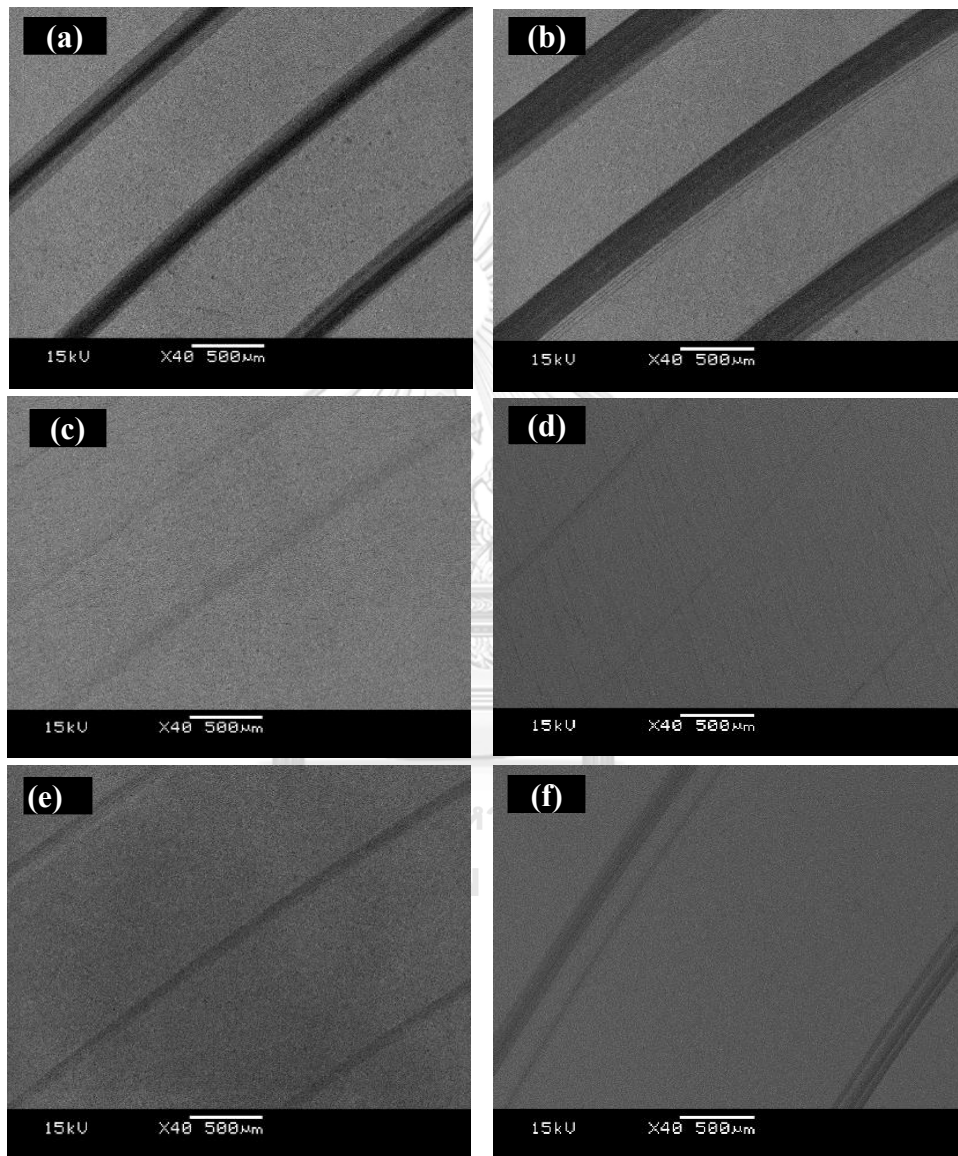


**Fig. 4.4** Electron micrographs of AlTiC surface after tribological measurements under surface condition and force of (a) dry surface at 0.1 N, (b) dry surface at 0.5 N, (c) lubricated with EG-based lube at 0.1 N, (d) lubricated with EG-based lube at 0.5 N, (e) lubricated with oil-based lube at 0.1 N, and (f) lubricated with oil-based lube at 0.5 N. Note that all the samples were from the sliding speed of 3600 mm/min.

For the dry surface condition, the deep wear tracts were observed on the surface as the normal force was used at 0.1 N. The wear tracts became wider but seemingly less deep as the normal force was increased to 0.5 N. Much shallower wear tracts can be observed as the EG-based lubricant was used, leading to an order of magnitude reduction of COF values, as seen in Fig. 4.2. It can be explained as the friction during the measurement belonged to the mixed friction regime and the hydrodynamic regime, as seen before in Fig. 4.3 (b). Larger and deeper wears (although not as deep as those obtained from the dry surface condition) were also been observed as the oil-based lubricant was used. This may be due to the fact that the friction regime in the oil-based lubricant case belonged to the mixed friction regime at the exerted normal force of 0.1 N and transferred to the boundary friction regime, as the normal force was increased for 5 times (up to 0.5 N).

## 4.2 Effects of additives in an EG-based lubricant on the friction regime

The major benefit of adding additives into the base lubricant is to achieve additional functions for a better performances lubricant. For example, corrosion inhibitors can help to prevent the corrosion of metals or materials during lapping process. The surfactant additive helps not only reduce the viscosity but also capture the debris during lapping process. Apart from the chemical effects on the final lapping process, the effects on the friction regime during the process of both corrosion inhibitor and the surfactant were investigated using the tribometer with the additive modified EG-based lubricants. Different types of additives were mixed into the EG-based lubricant and then lubricated on the AlTiC wafer. Then, the friction force was measured, and the COF values were calculated. All the modified lubricants contained 92-93 % wt. of ethylene glycol. As discussed earlier in section 4.1, the normal force used in this experiment was set at 0.5 N. The calculated COF values as a function of sliding speed are presented in Fig. 4.5 for further discussion.

### 4.2.1 Effects of surfactants in the EG-based lubricants on the friction force

The COF values as a function of sliding speed obtained from experiment where utilized different surfactants-modified EG-based lubricants, were displayed in Fig. 4.5. The notation, chemical names, as well as the weight percentage compositions of the surfactants were presented in Table 3.2.

The present of the surfactants can slightly increase the values of COF. As seen from Fig. 4.5, the calculated COF were independent from an increasing of sliding speed. This implied that the friction regime was in the boundary friction regime. Scanning electron micrographs of the AlTiC surfaces after measurement were presented in Fig. 4.6. A comparison of wear tracts between the use of EG-based lubricant and modified EG-based lubricants indicated that the presence of the surfactants can slightly induce wears. This could be due to the friction was belonged to the boundary friction regime for all employed sliding speed. Another possible cause was the decreasing of the surface tension in liquid phase, caused by the surfactant and

decreasing the lubricant thickness. Further experiment to determine the contact angle and, hence, the change in the surface tension, is required and suggested.

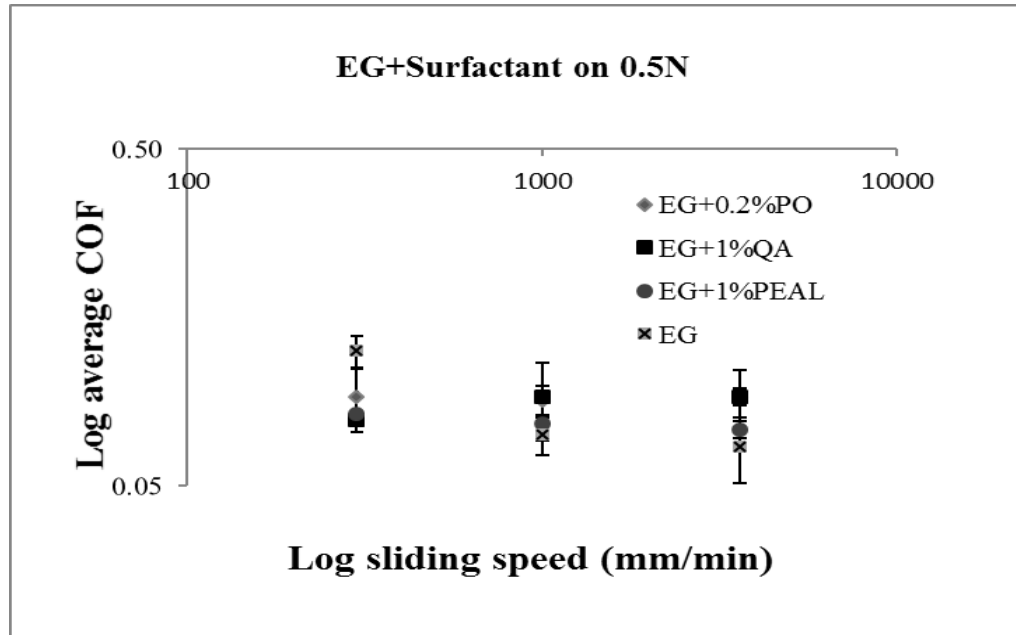


**Fig. 4.5** Graph log-scale plot of EG- and surfactant-modified lubricants on AlTiC disk sliding against SUS304 ball at 0.5N with various sliding speed

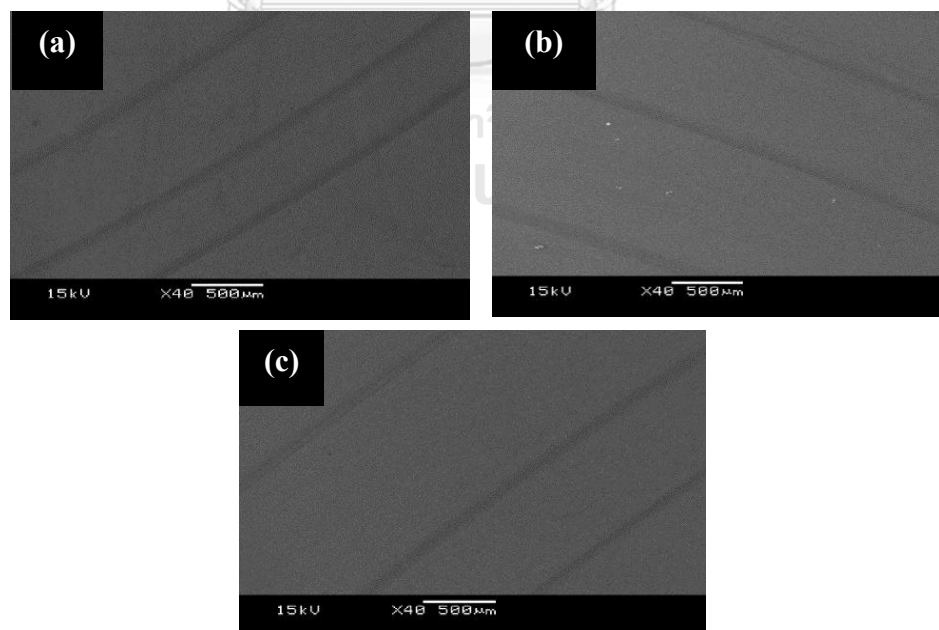


**Fig. 4.6** Electron micrographs of wears on AlTiC surfaces after tribology measurement with surfactant (a) PO, (b) QA and (c) PEAL modified lubricants

#### 4.2.2 Effects of corrosion inhibitor in the EG-based lubricants on the friction force.

The COF values obtained from the measurement using EG-based lubricants mixed with corrosion inhibitor as a function of sliding speed were shown in Fig. 4.7. The notation, chemical names and composition of the lubricants with corrosion inhibitors were presented in Table 3.2.

In contrast with the effects from the presence of additional surfactant, the presence of the corrosion inhibitor seems to decrease the value of COF. The COF obtained from the measurement, using corrosion inhibitors mixed EG-based lubricant declined as a function of sliding speed. The COF dropped as a function of sliding speed with  $\text{COF} \propto v^{-0.52}$  and  $\propto v^{-0.44}$  as the inhibitor corrosion was PG and PO, respectively. The calculated power law relationship is close to that predicted, as the  $\text{COF} \propto v^{-1/2}$  in the mixed friction regime. However, there is a concern on the results with PO additive. Thus, PO can act both a corrosion inhibitor and a surfactant. With a small amount of 0.06 %wt., it played as corrosion inhibitor whereas 0.2%wt. was founded as surfactant role.

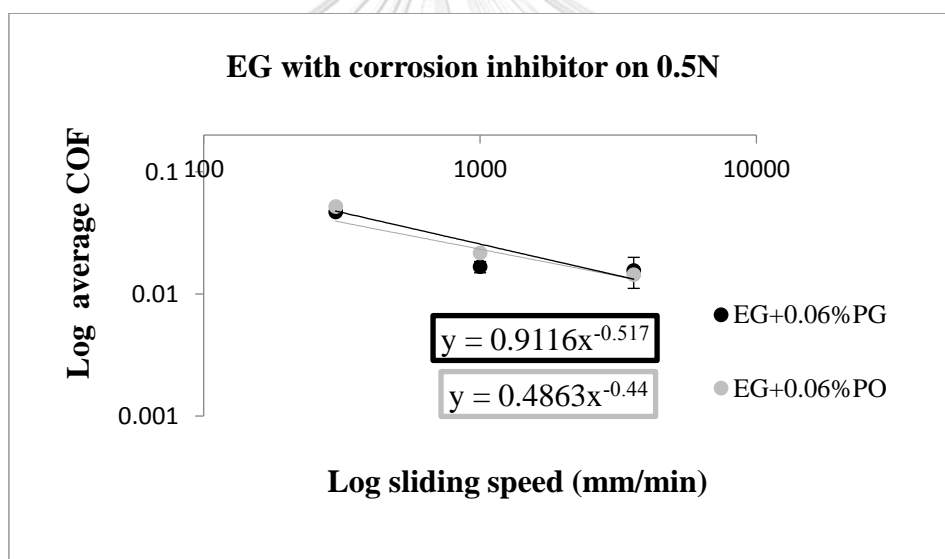


**Fig. 4.7** Graph log-scale plot between sliding speed and average COF of EG-based lubricant mixed with corrosion inhibitor

#### 4.2.3 Effect of a combination of surfactants and corrosion inhibitors in an EG-based lubricant on the occurred friction.

The COF values as a function of sliding speed from the measurement, using EG-based lubricants modified with both surfactants and corrosion inhibitors were shown in Fig. 4.8. The measured results, using lubricants containing both surfactant and corrosion inhibitor were quite similar to the case that using the lubricant containing



only corrosion inhibitor. This result points out that the corrosion inhibitor dominated the friction process, in spite of a very small amount of it being added into the base lubricant. The obtained COF from an experiment with EG-based lubricant contained both surfactant and corrosion inhibitor, decreased as a function of sliding speed. The COF changed as a function of sliding speed with  $\text{COF} \propto v^{-0.42}$  and  $v^{-0.491}$ , as the corrosion inhibitor was PG and PO, respectively. The calculated power relationship was close to the mixed friction regime.

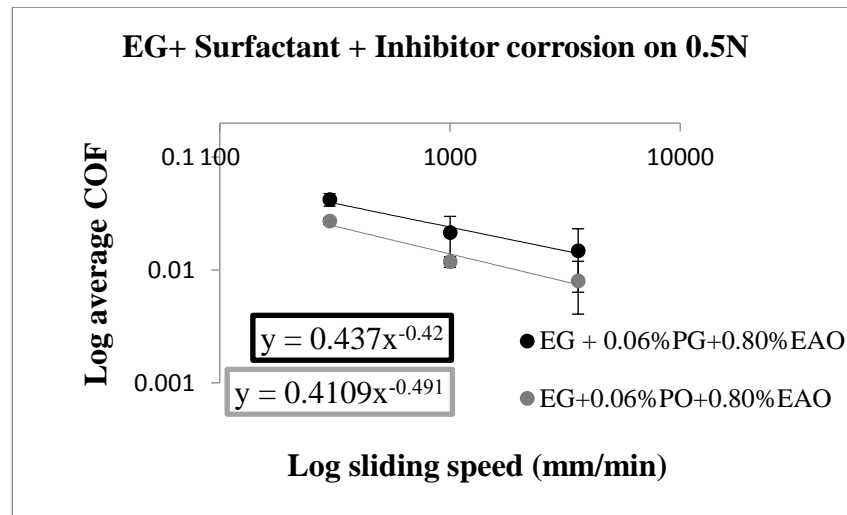


**Fig. 4.8** Graph log-scale plot between sliding speed and average COF of EG based lubricant with both corrosion inhibitor and surfactant

The COF of EG-based lubricant with only surfactant at load of 0.5N and sliding speed of 3600 mm/min was approximate 0.70-0.90. It was too large to compare with those corrosion-inhibitor-modified lubricants and both surfactant-corrosion-inhibitor-modified lubricants, which were in the range of 0.014-0.150, and 0.008-0.015, respectively.

## CHAPTER V

### CONCLUSIONS AND SUGGESTIONS

The friction characteristics and regimes of lubricated AlTiC surfaces were investigated, using AUS304 steel ball sliding against the AlTiC wafer at various load forces, sliding speeds and different types of lubricant. All the tribological studies were done by using ball-on-disk tribometer which the COF values were extracted from the measurements. For the dry surface (no lubricant), the COF value was increased as the normal load force increased, but independently from the sliding speed. For dry surface, the lubricant behavior was founded in boundary regime, which the lubricant thickness is much less than the surface roughness at the sliding contact point. This dry surface case gave the highest COF values. For EG-based lubricated AlTiC surface, the COF values depended on the sliding speed. That implied the EG-based lubricant behavior can be in different friction regimes, compared to dry surface. At small load force of 0.1 N, an average COF (after 100 contact cycles) implied that the EG-lubricant behavior belonged to the mixed regime at small sliding speed and then transformed to the hydrodynamic regime at higher sliding speed. The COF before 100 contact cycles cannot be measured due to the measured values were very small. Since the COF values were very small, we cannot confirm the lubricant regime. It is possible that it will belong to hydrodynamic regime. However, the ball-on-disk tribometer experiment, investigate the wear occurrence during the first 100 contact cycles using SEM in order to confirm the accuracy of COF measurement, is suggested in the future study. For at higher load 0.5 N, the EG-based lubricant behavior changed from a mixed regime to boundary regime. In contrast with the oil-based lubricants, their COF decreased as the sliding speed increased at the load force of 0.1 N. However, at 0.5 N, the COF is independent on the sliding speed. The different normal load forces led to different friction regimes. SEM investigation showed the wears have occurred by oil-based lubricant more than EG-based lubricant. It also found that the mechanism of wear was an abrasive wear.

Although the EG-based and oil-based lubricants were both in the liquid phase, the friction characteristics and friction regimes once the lubricants were employed were found to differ. In addition, the viscosity of EG-based lubricant (at 20 cP) was almost 10 times higher than the viscosity of the oil-based lubricant (at 1.68 cP). Nevertheless, this did not lead to significant difference of the COF values.

Moreover, the study of effects of added functional additives into EG-based lubricant was performed. There were 2 types of functional additives used in this study; the surfactants and the corrosion inhibitors. (Some of the additives can be classified as both.) The addition of surfactant led to the COF values being independent of the ball sliding speed, implying that the occurred friction belongs to the boundary regime. On the other hands, adding corrosion inhibitors leads to the friction being in the mixed regimes; a similar effect was observed when both surfactant and corrosion inhibitor were added into the base lubricant. However, the explanation regarding the effect of the PO additive remains unclear; at a small concentration of 0.06% wt, the observed behavior of the friction at the lubricated surface is the same as the other corrosion inhibitor which is that of the friction in the mixed regime. However, when it was added

into the lubricant at larger weight percentage (0.2%wt), the friction characteristic was found to be similar to that of friction between surfaces covered with EG-based lubricants implemented with surfactants; the friction belonged to a boundary regime.

Further investigations regarding the effects of the concentration of additives in lubricants on the friction force are still required. Moreover, an investigation the effect of additive concentrations on the friction characteristic by focusing on the impacts of wettability on the COF is suggested for fully understanding. Finally, studying on the gap between load force that exerted on the surface as 0.1-0.5 N is recommended on both EG-based and oil-based lubricants.



## REFERENCES

1. Fu Y. Tribological Study of Contact Interfaces in Hard Disk Drives University of California; 2016.
2. GROCHOWSKI E. Emerging Trends in Data Storage on Magnetic Hard Disk Drives.11-6.
3. Djamal M, Ramli. Development of Sensors Based on Giant Magnetoresistance Material. *Procedia Engineering*. 2012;32:60-8.
4. Wannasin APDJ. Hand book of the final process2013.
5. Lapping Process [cited 2018 29 June 18]. Available from: <https://en.wikipedia.org/wiki/Lapping>
6. Aihua L, Jianxin D, Haibing C, Yangyang C, Jun Z. Friction and wear properties of TiN, TiAlN, AlTiN and CrAlN PVD nitride coatings. *International Journal of Refractory Metals and Hard Materials*. 2012;31:82-8.
7. Zhou F, Wang Y, Ding H, Wang M, Yu M, Dai Z. Friction characteristic of micro-arc oxidative Al<sub>2</sub>O<sub>3</sub> coatings sliding against Si<sub>3</sub>N<sub>4</sub> balls in various environments. *Surface and Coatings Technology*. 2008;202(16):3808-14.
8. Ding H, Dai Z, Zhou F, Zhou G. Sliding friction and wear behavior of TC11 in aqueous condition. *Wear*. 2007;263(1):117-24.
9. Stachowiak GW, Batchelor AW. 1 - Introduction. In: Stachowiak GW, Batchelor AW, editors. *Engineering Tribology (Third Edition)*. Burlington: Butterworth-Heinemann; 2006. p. 1-9.
10. Stachowiak GW, Batchelor AW. 10 - Fundamentals of Contact Between Solids. In: Stachowiak GW, Batchelor AW, editors. *Engineering Tribology (Third Edition)*. Burlington: Butterworth-Heinemann; 2006. p. 461-99.
11. Introduction to the Basics of Tribology Bruker 2013 [updated 3 April 2013; cited 2018 29 June 2018]. Available from: [https://www.bruker.com/fileadmin/user\\_upload/-PDF-Docs/SurfaceAnalysis/TMT/Webinars/Tribology\\_101\\_2-Characterize-the-Tribosystem\\_3-April-2013.pdf](https://www.bruker.com/fileadmin/user_upload/-PDF-Docs/SurfaceAnalysis/TMT/Webinars/Tribology_101_2-Characterize-the-Tribosystem_3-April-2013.pdf).
12. Bikiranjit Basu MK. *Tribology of ceramics and composition: WILEY*; 2011 Oct 2011.
13. Rebai H. *Tribology and machine elements: University of applied science*; 2014.
14. Shizhu Wen PH. *Principles of Tribology*. 2nd ed. Tsinghua University Press2017.
15. Gleghorn JP, Bonassar LJ. Lubrication mode analysis of articular cartilage using Stribeck surfaces. *Journal of Biomechanics*. 2008;41(9):1910-8.
16. viscosity 2018 [updated 9 July 201829 June 2018]. Available from: <https://en.wikipedia.org/wiki/Viscosity>.
17. Kietzig A-M, Hatzikiriakos SG, Englezos P. Physics of ice friction. *Journal of Applied Physics*. 2010;107(8):081101.
18. Oksanen P, Keinonen J. The mechanism of friction of ice. *Wear*. 1982;78(3):315-24.
19. company B. *CETR-UMT Hardware Installation and Application Manual*. Campbell USA: Center For Tribology; 2009.

20. Introduction to the UMT TriboLab 2015 [updated 05 07 2015; cited 2018 15 July]. Available from: [https://www.bruker.com/fileadmin/user\\_upload/8-PDF-Docs/SurfaceAnalysis/TMT/Webinars/TriboLabWebinar - 2015-05-07.pdf](https://www.bruker.com/fileadmin/user_upload/8-PDF-Docs/SurfaceAnalysis/TMT/Webinars/TriboLabWebinar - 2015-05-07.pdf).
21. Mishra T. Tribological Studies on Coating-Lubricant Combinations in Different Contact Configurations: Luleå University of Technology; 2015.
22. Shi Y, Minami I, Grahn M, Björling M, Larsson R. Boundary and elastohydrodynamic lubrication studies of glycerol aqueous solutions as green lubricants. *Tribology International*. 2014;69:39-45.
23. Hua M, Xicheng W, Jian L. Friction and wear behavior of SUS 304 austenitic stainless steel against Al<sub>2</sub>O<sub>3</sub> ceramic ball under relative high load. *Wear*. 2008;265(5):799-810.
24. Cho C-W, Lee Y-Z. Effects of oxide layer on the friction characteristics between TiN coated ball and steel disk in dry sliding. *Wear*. 2003;254(3):383-90.
25. Pereira J, Zambrano J, Licausi M, Tobar M, Amigó V. Tribology and high temperature friction wear behavior of MCrAlY laser cladding coatings on stainless steel. *Wear*. 2015;330-331:280-7.
26. Majdoub F, Belin M, Martin JM, Perret-Liaudet J, Kano M, Yoshida K. Exploring low friction of lubricated DLC coatings in no-wear conditions with a new relaxation tribometer. *Tribology International*. 2013;65:278-85.
27. Quinchia LA, Delgado MA, Reddyhoff T, Gallegos C, Spikes HA. Tribological studies of potential vegetable oil-based lubricants containing environmentally friendly viscosity modifiers. *Tribology International*. 2014;69:110-7.
28. Khan J. A lapping and polishing process to achieve high quality alumina surfaces for applications in device fabrication. *Thin Solid Films*. 1992;220(1):222-6.
29. Godfrey D. Friction oscillations with a pin-on-disc tribometer. *Tribology International*. 1995;28(2):119-26.
30. 3 - Fundamentals of contact mechanics and friction. In: Chen G, editor. *Handbook of Friction-Vibration Interactions*: Woodhead Publishing; 2014. p. 71-152.
31. Park S-S, Cho C-H, Ahn Y. Hydrodynamic analysis of chemical mechanical polishing process. *Tribology International*. 2000;33(10):723-30.
32. Meozzi M. Special use of the ball on disc standard test. *Tribology International*. 2006;39(6):496-505.
33. Zhou F, Wang X, Adachi K, Kato K. Influence of normal load and sliding speed on the tribological property of amorphous carbon nitride coatings sliding against Si<sub>3</sub>N<sub>4</sub> balls in water. *Surface and Coatings Technology*. 2008;202(15):3519-28.
34. Bandeira AL, Trentin R, Aguzzoli C, Maia da Costa MEH, Michels AF, Baumvol IJR, et al. Sliding wear and friction behavior of CrN-coating in ethanol and oil-ethanol mixture. *Wear*. 2013;301(1):786-94.
35. Khurshudov A, Waltman RJ. Tribology challenges of modern magnetic hard disk drives. *Wear*. 2001;251(1):1124-32.
36. Paranusorn P, Fernandez BL, Supavasuthi C, Somwangthanaroj A. Effects of Additives in Ethylene Glycol-based Lubricant on Selective Material Removal in Slider Lapping Process. *Procedia Chemistry*. 2016;19:166-73.

37. Nguyen PTM, Bhandari B, Prakash S. Tribological method to measure lubricating properties of dairy products. *Journal of Food Engineering*. 2016;168:27-34.
38. Gatzert HH, Beck M. Tribological investigations on micromachined silicon sliders. *Tribology International*. 2003;36(4):279-83.
39. Wood R. Future hard disk drive systems. *Journal of Magnetism and Magnetic Materials*. 2009;321(6):555-61.
40. Abdullah Tasdemir H, Wakayama M, Tokoroyama T, Kousaka H, Umehara N, Mabuchi Y, et al. Wear behaviour of tetrahedral amorphous diamond-like carbon (ta-C DLC) in additive containing lubricants. *Wear*. 2013;307(1):1-9.
41. Mahato A, Perry TA, Jayaram V, Biswas SK. Pressure and thermally induced stages of wear in dry sliding of a steel ball against an aluminium–silicon alloy flat. *Wear*. 2010;268(9):1080-90.



**APPENDIX**



จุฬาลงกรณ์มหาวิทยาลัย  
**CHULALONGKORN UNIVERSITY**

## VITA

Miss Sawanee Jitphayomkun was born on November 23, 1991. Her hometown is 9, Moo 1, Bangrakum, Photong, Anghong, Thailand 14120. She received the bachelor degree from Department of Physics, Faculty of Science, Chulalongkorn University in 2013. Then she was entranced to the master degree program in the same field and university and completed the program in 2017.

Here are her contact info; email [sa\\_wa\\_nee\\_tong@hotmail.com](mailto:sa_wa_nee_tong@hotmail.com) and mobile number is +66 988964142

